

Electron nanodiffraction and high-resolution electron microscopy studies of the structure and composition of physiological and pathological ferritin

C. Quintana,^{a,*} J.M. Cowley,^b and C. Marhic^c

^a Instituto de Microelectrónica de Madrid. C.S.I.C., 8 Isaac Newton, PTM, 28760 Tres Cantos Madrid, Spain

^b Arizona State University, Box 871504, Tempe, AZ 85287-1504, USA

^c Institut de Matériaux de Nantes, C.N.R.S., 2 rue la Houssinière, BP 32229, 44322 Nantes Cedex 03, France

Received 15 December 2003, and in revised form 26 February 2004

Available online 20 March 2004

Abstract

Structures of core nanocrystals of physiological (horse spleen, human liver, and brain) and pathological human brain of patients with progressive supranuclear palsy (PSP) and Alzheimer's disease (AD) ferritin molecules were determined using electron nanodiffraction and high-resolution transmission electron microscopy. The poly-phasic structure of the ferritin cores is confirmed. There are significant differences in the mineral composition between the physiological and pathological ferritins. The physiological ferritin cores mainly consist of single nanocrystals containing hexagonal ferrihydrite (Fh) and hematite (Hm) and some cubic magnetite/maghemite phase. In the pathological cores, Fh is present but only as a minor phase and Hm is absent. The major phases are a face-centered-cubic (fcc) structure with $a = 0.43$ nm and a high degree of disorder, related to wustite, and a cubic magnetite-like structure. These two cubic phases are also present in human aged normal brain. Evidence for the presence of hemosiderin together with ferritin in the pathological brains is deduced from the similarities of the diffraction patterns with those from patients with primary hemochromatosis, and differences in the shapes and protein composition of the protein shell. These findings suggest a disfunction of the ferritin associated with PSP and AD, associated with an increase in the concentration of brain ferrous toxic iron. © 2004 Elsevier Inc. All rights reserved.

Keywords: Ferritin; Ferritin cores nanocrystals; Hemosiderin; Progressive supranuclear palsy; Alzheimer diseases; HRTEM; Electron nanodiffraction

1. Introduction

Iron is a chemical element that plays an essential role in several important biological processes such as oxygen transport, electron transfer, and different enzymatic reactions. Nevertheless an excess of free iron is toxic for cells and for this reason living organisms have developed mechanisms to store the iron in a non-toxic form. Ferritin, the main molecule involved in iron storage (which accounts for storage of more than 90% of non-heme iron in redox-inert forms, Fe^{3+}), is a globular protein of about 12 nm in diameter with a central cavity—the core about

6 nm in diameter where iron is stored as hydrated, iron oxide, nanocrystals. The protein shell is made of 24 subunits, which are distinguished as either a heavy-chain (H) or light-chain (L) isoform that are genetically and functionally distinct. The H subunit has a specific ferroxidase activity for rapid iron uptake and the L subunit is involved in the nucleation and stabilization of nanocrystals (Harrison and Arosio, 1996). The mechanisms of uptake and oxidation of ferrous Fe^{2+} ion, nucleation and growth of iron oxide nanocrystals in the cores, reduction and release of iron from the molecule was reviewed by Massover (1993) and by Chasteen and Harrison (1999).

Identification of the mineral phase in the ferritin cores was performed in the 1960s, mainly by X-ray diffraction (XRD) and electron diffraction (ED) on *a set* of molecules. At that time, the currently accepted mineral composition was similar to the natural mineral

* Corresponding author. Present address: Institut Curie Recherche, Laboratoires Raymond Latarjet Centre Universitaire, Bat.112 F 91405-Orsay Cédex France. Fax: +33-1-69-07-53-27.

E-mail address: carmen.quintana@curie.u-psud.fr (C. Quintana).

described as “amorphous and paracrystalline-to-crystalline compounds of hydrous ferric oxide or ferric hydroxide called ferrihydrite (Fh),” Towe and Bradley (1967). Several models of structure were proposed by Harrison et al. (1967) and Brady et al. (1968).

Two decades later (Drits et al., 1993; Eggleton, 1988; Jambor and Dutrizac, 1998) ferrihydrite raised industrial interest and led to the synthesis and analysis of new preparations of Fh to be studied by other techniques as: EXAFS (Manceau and Drits, 1993), XANES, and Mössbauer spectroscopy, isotopic exchange and structural modeling of nanodiffraction patterns (for a review, see Jambor and Dutrizac (1998) and Janney et al. (2000a,b, 2001)). At present, the most common accepted model of Fh is the presence of at least three phases, the ratio of these three different structures varying from sample to sample. Recent studies of synthetic Fh by electron nanodiffraction (Janney et al., 2000b) also show new phases that vary according to the sample preparation method (a highly disordered material, a magnetite/maghemite like structure and a “double” hexagonal” structure with a hexagonal unit cell $a = 0.30$ nm (or 0.52 nm), $c = 0.94$ nm).

The new studies on Fh demand a revision of the structure of ferritin cores obtained using updated techniques for nanoanalysis, such as electron nanodiffraction (END) (Cowley et al., 2000; Isaacson and Ohtsuki, 1980; Quintana et al., 1987), high-resolution transmission electron microscopy (HRTEM) (Mann et al., 1986; Quintana et al., 2000; St. Pierre et al., 1989) and electron energy loss spectroscopy (EELS) (Quintana et al., 2000). These techniques that are currently used for nanoanalysis in Materials Science are little known and used in Life Sciences; they allow the analysis of individual ferritin cores. In 2000, two separate studies, performed using HRTEM and END, reported the polyphasic structure of the ferritin cores of horse spleen (Cowley et al., 2000; Quintana et al., 2000): a mixture of “classic” ferrihydrite (Towe and Bradley model) and other phases, including the presence of a cubic magnetite/maghemite like phase. The presence of more than one crystalline phase agrees with the results of Brooks et al. (1998) on the magnetic behavior of ferritin. This polyphasic structure of the cores could represent different forms of iron storage, one more stable form and another more labile form, and can be related to physiological state of the molecule.

In the normal brain, the iron is the more abundant metal and its concentration increase with age until approximately age 40. Iron has a specific regional and cellular distribution (Morris, 1992). On the other hand the hypothesis that some mishandling of the iron metabolism in human brain can be involved in the onset of some neurological disease has been recently reviewed by Burdo and Connor (2003) and Ke and Qian (2003). This hypothesis is supported by the following observations: (1) The presence of abnormally high iron levels in brain areas

which take part in several neurodegenerative disorders including Hallervorden–Spatz syndrome, Parkinson disease (PD), Alzheimer disease (AD), Pick disease, progressive supranuclear palsy (PSP), Huntington disease (HD) (Bartzokis et al., 1999; Dexter et al., 1991; Sayre et al., 2000). (2) The disruption expression of iron metabolism proteins, induced by genetic or non-genetic factors, is the cause of the increased brain iron (Connor et al., 2001; Qian and Shen, 2001; Sampietro et al., 2001).

In the cited preliminary study by HRTEM (Quintana et al., 2000) we have analyzed the core composition of human brain ferritin isolated from PSP and AD patients. An increase was found of magnetite/maghemite phase in these “pathological” ferritin cores. We suggest that the formation, inside of cores, of magnetite, in which ferric and ferrous ions are both present, would indicate a mishandling of the enzymatic oxidation of iron by ferritin. Ferritin with a higher amount of magnetite nanocrystals could release ferrous ions more easily outside of the protein. The ferrous ions may contribute to the production of free hydroxyl radicals and neural cell degeneration (Smith et al., 1997). For this reason the knowledge of the different phases present in the ferritin core nanocrystals might be of biomedical interest if the difference between the patterns found in physiological and pathological conditions is confirmed.

On the other hand, Kirschvink’s groupe (Kirschvink et al., 1992) and Dobson’s group (Dobson and Grassi, 1996; Dunn et al., 1995; Dobson, 2001; Hautot et al., 2003; Schultheiss-Grassi and Dobson, 1999) have reported the presence of biogenic magnetite in brain of normal individuals and in the hippocampus of patients suffering of mesial temporal lobe epilepsy (MTLE) and Alzheimer disease. Dunn et al. (1995) indicates, “that if the magnetite in the brain is simply a by-product of iron metabolism, its accumulation may be important in pathological conditions commonly associated with aging.” Dobson (2001) suggests that the magnetite crystals inside the ferritin may act as a precursor for the formation of biogenic magnetite in brain. Also, the results from Hautot et al. (2003) indicate that levels of magnetite are higher in AD brain tissues when compared to aged-matched normal tissue.

In this paper, we describe new results concerning the composition of core nanocrystals of physiological and pathological ferritins. We have used electron nanodiffraction and high-resolution electron microscopy to identify the mineral phases of nanocrystals forming the ferritin cores. We have studied a greater number of cores proceeding from two different commercial sources of horse spleen ferritin, from commercial human liver ferritin, and from brain of patients of PSP and AD. Also, ferritin present in sections of cerebral cortex removed during autopsy in a normal aged human brain and in sections of caudate nucleus of one of the PSP patients were analyzed.

The polyphasic structure of all the analyzed ferritin cores is confirmed and quantified. The physiological horse spleen and human liver ferritin cores contain mainly ferrihydrite (Ft), hematite (Hm), and some cubic magnetite/maghemite-like phase. In pathological PSP and AD ferritin cores, Fh is present but only as a minor phase and Hm is absent; the major phases are a face-centered cubic (fcc) structure with $a = 0.43$ nm and with a high degree of disorder, related to wüstite, and a cubic magnetite-like structure. The aged normal human brain ferritin cores contain the same proportion of Fh as the horse spleen and human liver ferritin cores and similar proportion of fcc structure, $a = 0.43$ nm, as the pathological one. Furthermore, we also found significant differences in the morphology and peptide composition of the protein shell in the isolated pathological ferritin.

In spite of the small number of patients studied, the set of differences found in the cores and in the protein shell leads us to suggest that in the brain of PSP and AD patients there is, besides ferritin, a form of hemosiderin similar to that found in primary hemochromatosis. This hypothesis is supported for the “in situ” localization of hemosiderin at ultrastructural level in caudate nucleus of the a PSP patient

2. Materials and methods

2.1. Sample preparation

Commercial horse spleen (Calbiochem and Sigma) and human liver ferritin (Calbiochem) were used. The solution was diluted at 1:100 in water and a drop of this diluted solution was placed on a carbon-coated copper or titanium grid and then examined by HRTEM and nanodiffraction.

Isolation of brain ferritin associated to the tau filaments in PSP and in AD patients was performed using the Greenberg and Davies (1990) procedure for paired helical filaments (PHF)-tau isolation as previously described (Perez et al., 1998). The Netherlands Hersen Bank (Dr. Ravid) provided us with one of the sample from PSP patients as well as the aged brain control samples from healthy subjects. A drop of the undiluted solution was placed on a carbon-coated copper, nickel or titanium grid and then examined by HRTEM and nanodiffraction.

Fresh-frozen fragments of caudate nucleus of one PSP subject and fragments of cerebral cortex of one aged healthy subject were fixed at room temperature for 12 h in a solution of 1% glutaraldehyde, 4% paraformaldehyde, in 0.4 M Hepes buffer. At this short time-scale the fixatives have no effect on the leaching of iron oxides (Dobson and Grassi, 1996).

Samples were postfixated with 1% OsO₄ during 1 h at 4 °C, rinsed in the Hepes buffer, dehydrated in graded

series of acetone, and embedded in Epon resin at 60 °C during 48 h. Conventional sections of 40–60 nm were obtained and directly collected on copper or gold grids. For structural studies the sections were lightly stained with uranyl acetate 2% in water for 30 s.

2.2. Techniques

2.2.1. Identification of mineral phase in individual nanocrystals

Identification of the mineral phase of an individual crystal can be performed by measuring crystallographic parameters. These data can be obtained in a transmission electron microscope (TEM) from direct measurements of periodicities of lattice fringes observed in high-resolution TEM images (HRTEM) or from END.

(a) Crystallographic data from HRTEM and Fourier transform (FT).

HRTEM recorded under specific conditions of defocus are closely related to the projection of the atomic potential distribution of the crystal and it can be considered that the periodicities of interference fringes represent the lattice spacing. The measurement of fringe periodicities in HRTEM can be more precisely performed by computing the numerical FT of HRTEM images.

In some cases identification of the phase of a nanocrystal, oriented with a simple zone axis parallel to the electron beam, can be performed. In such cases, the HRTEM images show at least two systems of fringes from which two lattice spacing can be derived. If the measured lattice spacing differ from one phase to the other, then the identification is unambiguous.

(b) Crystallographic data from electron nanodiffraction.

In the dedicated STEM instrument, large numbers of nanodiffraction patterns from individual cores can be recorded rapidly. When a bright-field or dark-field image of high magnification is viewed on the display screen, an electronic marker is placed on the image of a ferritin molecule core. The beam is stopped at that point and the nanodiffraction pattern from the core is displayed on a TV monitor and either photographed directly or else stored on a video-cassette recorder (VCR), for future photography and analysis.

Typically, the beam diameter at the specimen level is 0.7 nm, and series of nanodiffraction patterns may be observed or recorded as the beam is translated across a core to detect any variations of structure. Since the crystallites in the ferritin cores come in arbitrary orientation, many nanodiffraction patterns come from non-axial orientations and are difficult to interpret. However, for those two-dimensional single-crystal patterns coming from crystallites which are close to an axial orientation, comparisons of the dimensions and relative

intensities with those for patterns calculated for known structures are usually sufficient to allow the phase to be identified without ambiguity.

Microanalysis of some individual ferritin cores was performed using EELS in a HB-501 dedicated STEM instrument, to give the compositions of the cores or else maps of the distribution of particular atoms within the cores with a spatial resolution of about 1 nm.

2.2.2. Biochemical analysis

Electrophoresis was carried out as previously described (García de Ancos, 1993) on 1-mm-thick 10% polyacrylamide slab gels. Immunoblot analysis was also done as previously described.

2.3. Instruments

An HRTEM 200-kV Hitachi HF2000-FEG was used to obtain high-resolution images at high magnification ($G = 7 \times 10^5$ and 1×10^6). The limiting point resolution obtained with this microscope is 0.13 nm. This microscope is equipped with a CCD Camera (MSC 794 Gatan). Electron nanodiffraction patterns were obtained with a dedicated scanning transmission electron microscope, the HB-5 from VG microscopes, specially modified for the observation and recording of electron nanodiffraction patterns and equipped with TV-VCR and CCD recording systems. EELS analysis of the particles in some specimens was performed with an HB-501 STEM instrument from VG Microscopes.

2.4. Experimental conditions

High-resolution images were digitally acquired with the CCD Camera at 1024×1024 or 512×512 pixels 2× bytes, using either an objective aperture of 160 μm , or without an aperture. The FT was computed with Digital Micrograph software version 2.5 on a Power Mac or with CRISP software on a PC after conversion to one byte. Calibrations of FT at several magnifications were made on high-resolution images using an Al sample. Pixel sizes were 0.0265 nm for $G = 7 \times 10^5$ and 0.0210 nm for $G = 1 \times 10^6$. Filtered images (inverse FT) were performed with CRISP software. The indexing of the power spectrum (PS) (square of the modulus) of the FT intensities (digital diffractogram) and the computation of diffracted intensities for each structural model of Fh were performed with the aid of Electron Diffraction software version 6.8 (Mornirolli, University of Lille) for PC.

2.4.1. Changes of structure induced by electron irradiation

For most biological and organic materials, and for some inorganic materials, irradiation by the incident electron beam in an electron microscope can change the structure, sometimes rendering crystalline material amorphous or, in other cases, changing the composition

and crystalline structure. It is therefore of primary concern to determine whether any such changes are occurring for the system studied.

For the iron oxide phases in ferrihydrite samples and ferritin cores, no changes of structure have been observed for any level of electron irradiation. The most intense irradiation of local specimen regions is given by the focused beam used for nanodiffraction. With such beams, changes in the diffraction pattern have been observed to take place within the first fraction of a second of irradiation for some minerals (e.g., clay minerals, silica) and over a period of several seconds for other inorganics. But for the iron oxide/hydroxide phases in ferritin cores, or in ferrihydrite samples, no changes are visible during continued irradiation for several minutes.

2.4.2. Contamination of samples with copper particles

For some ferritin samples, mounted on thin carbon films held on the copper grids commonly used for electron microscopy, there were regions containing many small particles of uniform size (5–6 nm) and shape which could readily be mistaken for ferritin cores. Electron nanodiffraction from these particles showed them to have a fcc structure with cell dimensions of about 0.365 nm (equal to those for copper or fcc iron). A small fraction of these particles showed a structure which appeared to be body-centered cubic (bcc) with cell dimensions about 0.28 nm (equal to that for bcc iron or for a bcc modification of copper). EELS analysis of these particles showed them to be copper.

Experiments with copper grids and thin carbon films in the absence of ferritin preparations, showed that distributions of small copper metal particles may occur, especially in the presence of protein or other organic material, presumably as a result of diffusion of copper from the grid wires. For one sample mounted on a gold grid it was found that some copper impurity had segregated to the surface of the gold and produced some small copper particles. One sample of ferritin mounted on a nickel grid showed a distribution of small metallic nickel particles, 2–3 nm in diameter. Preparations of ferritin mounted on titanium grids showed no evidence of any such particles or for any objects attributable to titanium or its compounds.

3. Results

3.1. Core nanocrystals of physiological ferritins

3.1.1. Horse spleen ferritin

To get a more extended analysis of horse spleen ferritin we analyzed HRTEM images of molecules from two different commercial sources (Calbiochem and Sigma). No significant differences were observed between the two types of preparations.

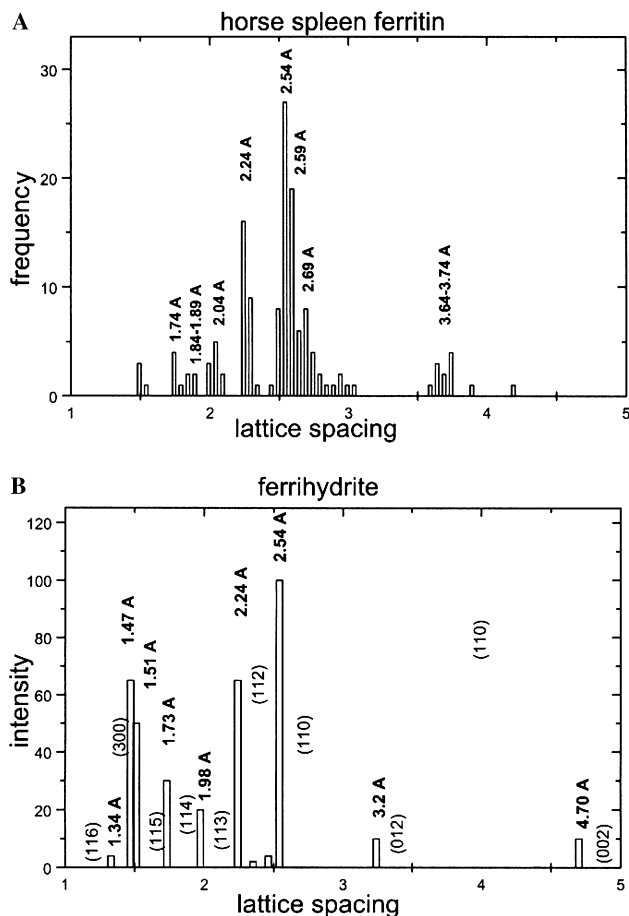


Fig. 1. Distribution of lattice spacing in nanocrystals. (A) Histogram corresponding to 141 values measured in horse spleen ferritin cores. (B) Schematic distribution of lattice spacing in ferrihydrite derived from X-ray diffraction data.

The average size of the nanocrystals was 5 nm. In these crystals, the distribution of the measured lattice spacing, d , (over a total of 141 values corresponding to 46 different cores) is shown in Fig. 1A. The distribution exhibits peaks at values of $d = 0.254, 0.224, 0.204$, and 0.174 ± 0.005 nm identified as $\{110\}$, $\{112\}$, $\{113\}$, and $\{114\}$ planes of Fh with lattice parameters $a = 0.508$ nm and $c = 0.94$ nm, or as $\{010\}$, $\{012\}$, $\{013\}$, and $\{014\}$ planes if the a -axis is taken as 0.296 nm. Other lattice spacing at 0.361 – 0.374 , 0.269 , and 0.184 – 0.189 nm can be identified as the lattice spacing corresponding to $\{012\}$, $\{014\}$, and

$\{024\}$ planes of hematite. There are some values around 0.3 nm that may correspond to $\{220\}$ planes of magnetite/maghemite.

3.1.2. Human liver ferritin

HRTEM images of commercial Calbiochem human liver ferritin were acquired and analyzed. The average size of the cores (about 6 nm in diameter) is bigger than that of horse spleen ferritin. As for horse spleen ferritin, the values of $d = 0.254, 0.223$, and 0.198 ± 0.005 nm (over a total of 91 values corresponding to 31 different cores) are the most common and they allow the phase identification as Fh. Other lattice spacing greater than 0.254 as 0.274 and 0.361 Å can be considered close to the lattice spacing of maghemite and hematite. These results show that, as in the horse spleen ferritin, cores of human liver ferritin are composed of three phases.

Of the 60 or so nanodiffraction patterns recorded from the sample of human liver ferritin, 41 could be attributed to known phases, as follows: 21 from the hexagonal phase of ferrihydrite, 10 from magnetite/maghemite, 3 from hematite, 2 from a fcc phase with $a = 0.43$ nm, showing evidence of considerable stacking disorder, and 2 each from a cubic phase with $a = 0.56$ nm (possibly NaCl) and an unknown hexagonal phase with $a = 0.35$ nm, which could possibly be the pseudo-hexagonal phase in 2-line ferrihydrite (Janney et al., 2000a). The relative proportions of these phases are very close to those previously observed (Cowley et al., 2000) for horse spleen ferritin. These results show that there are no significant differences between the composition of ferritin cores in horse spleen and human liver. The percentage of each phase is represented in Table 1.

Fig. 2 shows three examples of nanocrystals oriented near a zone axis together with their digital diffractogram and the theoretical diffraction patterns. Fig. 2A shows the most frequently found orientation corresponding to the $[00.1]$ zone axis of the Fh. Fig. 2D shows one nanocrystal of Fh oriented along the $[-11.0]$ axis and Fig. 2G shows one hematite nanocrystal oriented along $[48.-1]$ zone axis.

3.1.3. Human brain ferritin

Lightly stained sections of cerebral cortex of the aged brain control from a healthy subject were observed in a

Table 1
Phases in nanodiffraction patterns identified for various ferritin sources (%)

Phase	PSP patients	AD patients	Horse spleen and human liver	Aged human brain
6LFh hexagonal	17	15	53	49
Magnetite-like	30	30	30	20
fcc, $a = 0.43$ nm	38	50	5	29
Hematite	3	0	5	0
Minor phases	10	5	8	2

Note. The minor phases include goethite, lepidocrocite, an unknown hexagonal phase, possibly that in 2-line ferrihydrite, and a bcc phase with $a = 0.32$ nm.

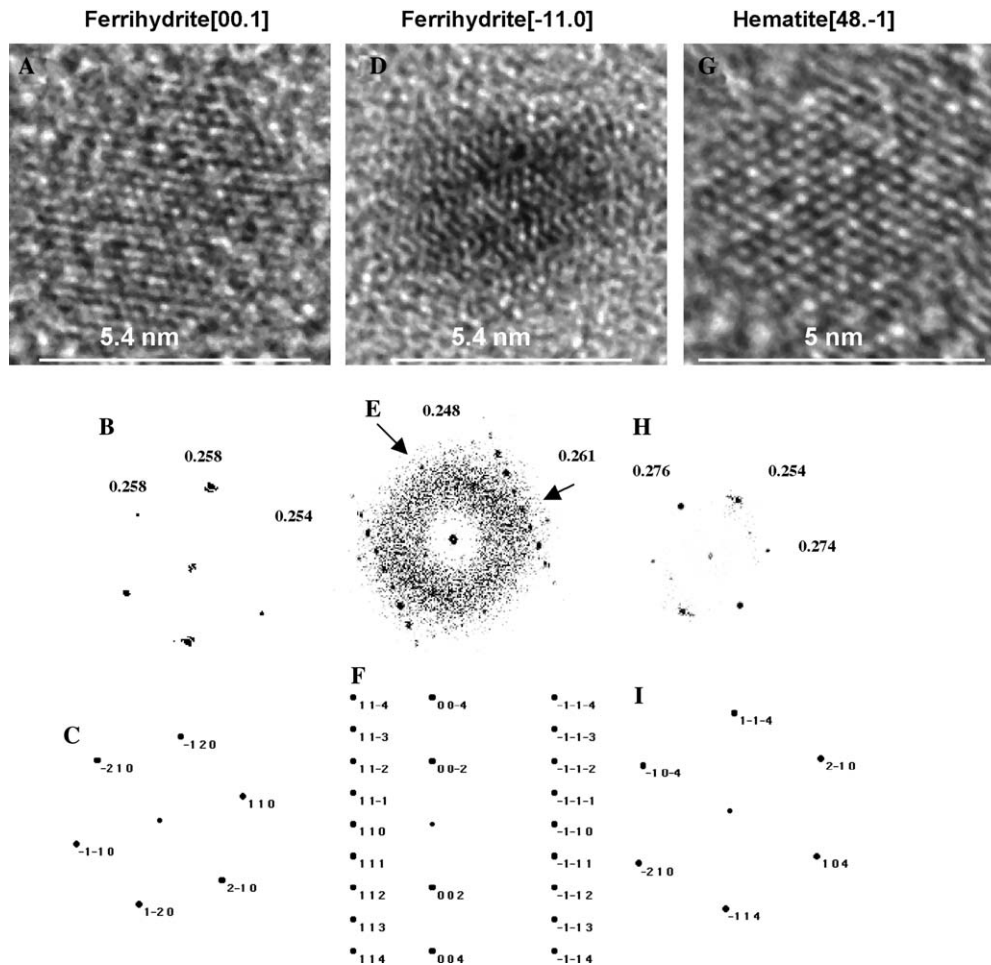


Fig. 2. Horse spleen and human liver ferritin. (A, D, and G) High-resolution TEM images of nanocrystal cores. (B, E, and H) Digital diffractogram obtained from numerical Fourier transform of the nanocrystals. (C, F, and I) Theoretical diffraction patterns.

conventional transmission electron microscope (CTEM) (Figs. 3A and B). Ferritin molecules are present in cytoplasm of cells and near to myelinic structures. Nanodiffraction patterns from ferritin cores performed on unstained sections showed that, as for the ferritin cores of horse spleen and human liver, the major phase is constituted by Fh. Magnetite/maghemite is also present and we found a greater proportion of the fcc phase with $a = 0.43$ nm.

3.2. Core nanocrystals of pathological ferritins

3.2.1. Human brain ferritin

The cores of brain ferritin in PSP and AD patients were studied by HRTEM and END. Low-resolution TEM images of unstained preparations obtained by following the procedure of Perez et al. (1998) shows ferritin molecules bound to Tau-filaments in PSP (Fig. 4A) and PHF in AD (Fig. 4B) and the presence of a number of unbound ferritin molecules.

Lightly stained thin sections of fragments of caudata nucleus from a PSP patient were observed in a CTEM

(Figs. 3C–E). In a preceding work (Perez et al., 1998) we have shown, at the histological level, that ferritin and Tau protein are co-localized in glial and neurones cells of caudate nucleus in PSP patients. Although the ultrastructure of brain tissues after autopsy is, generally not well preserved, the principal cellular constituents can be easily recognized. Ferritin is present in the cytoplasm and in the nucleus of neurones, principally in the nucleoplasm (Fig. 3D). In heterogeneous lysosomes of glial cells, ferritin, and cluster of hemosiderin are observed (Fig. 3E).

Ferritin cores in PSP were analyzed by HRTEM and END while ferritin cores in AD were analyzed only by END. The number of cores analyzed by HRTEM was 47 (210 measures of d) and 123 by END in PSP and 38 by END in AD.

For the 400 or more electron nanodiffraction patterns from PSP and AD samples which could be interpreted as coming from identifiable phases, more than one half were attributed to the fcc structure with $a = 0.37$ nm, approximately, or else the equivalent bcc structure with $a = 0.29$ nm, and these patterns were shown to come

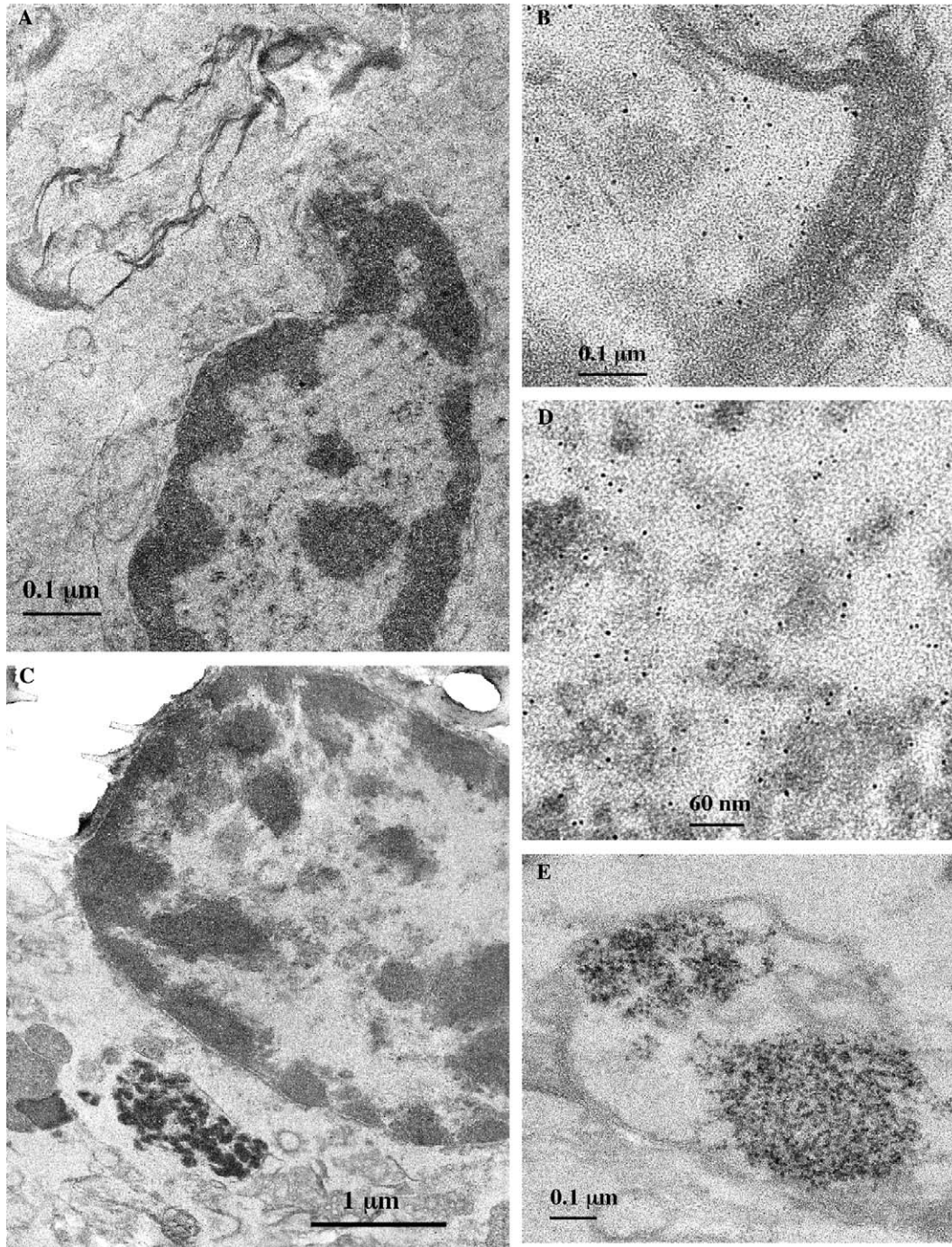


Fig. 3. TEM images of human brain ferritin. (A,B) Cerebral cortex of a healthy subject. (A) Stained section showing one well-conserved nucleus. (B) Other region at higher magnification showing some ferritin molecules near to myelinic structures. (C–E) Caudate nucleus of a PSP patient. (C) Stained section showing one well-conserved neuron nucleus. (D) Detail at higher magnification showing ferritin molecules in nucleoplasm. (E) Lysosome containing ferritin and hemosiderine in a glial cell.

from the contamination of the samples by copper particles from the copper grids used to support the specimens. Of the remainder of the patterns, it was evident that two-thirds or more came from either the fcc phase with $a = 0.43$ nm or else from the magnetite/maghemite structure. The hexagonal ferrihydrite phase was present in less than 20%. Minor phases, present in less than

about 5%, included hematite and goethite and there were a few patterns from unknown phases.

The relative percentages of their occurrence for specimens of ferritin from PSP and AD patients are listed in Table 1. There is a very clear difference from the relative occurrences of the phases in the “normal” ferritins from horse and human liver. The proportions

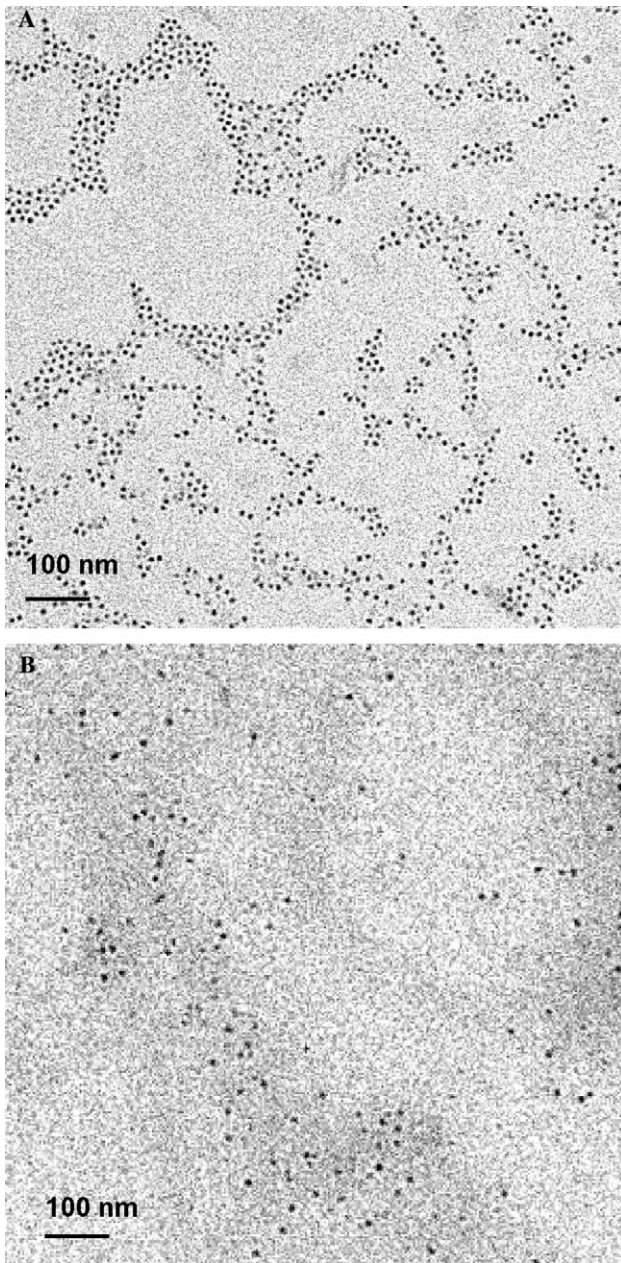


Fig. 4. Human brain ferritin extracted from patients with PSP and AD. (A) PSP ferritin associated to aberrant Tau filaments, unstained preparation (B) AD ferritin associated to PHF, unstained preparation.

of the hexagonal, 6LFh phase are much less than for the normal ferritins and the cubic, $a = 0.43$ nm phase is much more prominent, approaching 50%. Nanodiffraction patterns from the magnetite/maghemite phase and the fcc phase with $a = 0.43$ nm for various orientations are reproduced in Fig. 5. The continuous lines between the (1 1 1) and (2 0 0)-type spots, containing extra diffuse spots, in Fig. 5F are evidence for a high density of stacking faults on (1 1 1)-type planes.

It is remarkable that the values of lattice spacing 111(0.248 nm), 200(0.215 nm), and 220(0.152 nm) corresponding to the cubic, $a = 0.43$ nm phase are very near

to the lattice parameters present in electron diffraction patterns (0.249, 0.212, and 0.153 nm) from samples of hemosiderin obtained from liver of patients suffering primary hemochromatosis (Dickson et al., 1988; Mann et al., 1988). To test the presence of hemosiderin in our preparations, we studied the morphology and the peptide composition of the protein shell in the pathological ferritin brain extracted samples. Negatively stained preparations (Figs. 6A and B) show that some ferritin molecules have an irregular and/or incomplete shell around the cores. A biochemical characterization of human healthy (control) and PSP brain extracts was carried out. The presence of ferritin was confirmed by running a sample of each extract on electrophoresis gel and performing a Western blot analysis with the specific antibody. This analysis showed the presence of the major band at 20 kDa corresponding to ferritin in the control preparation and two bands at 20 and 15 kDa in the PSP patient; this band at 15 kDa can correspond to hemosiderin (Ward et al., 1994; Weir et al., 1984a) (results not shown)

4. Discussion

The earlier suggestion that ferritin cores from pathological origin could be structurally different from normal ferritin (Quintana et al., 2000) prompted us to make a more systematic analysis, using ferritins of different origin. We have used high-resolution TEM and electron nanodiffraction methods well known in Materials Science but little known in Life Science. These methods allow the analysis of the individual nanocrystals that compose the ferritin cores.

Our previous analysis of control physiological ferritin (Cowley et al., 2000; Quintana et al., 2000) was extended using two new commercial sources of horse spleen ferritin. We have also studied *human* ferritin; commercial liver and brain ferritin from a healthy subject.

The pathological ferritin cores extracted from the brains of patients suffering neurodegenerative diseases, come from the same patients previously studied (three PSP patients and four AD patients), (Quintana et al., 2000) and from a new PSP patient (Netherlands Hersen Bank). The number of measured cores *has been significantly increased*. We have also analyzed cores of ferritin present in the sections of caudate nucleus fragments, embedded in Epon, of the last new patient.

The results presented in this work show the similarity of the distribution of phases in the horse spleen and in the human liver ferritin. As in the case of natural mineral or synthetic ferrihydrite, the cores are built up by crystals of different structures. The main phase corresponds to an hexagonal structure with parameters $a = 0.296$ (or 0.51 nm) and $c = 0.94$ nm. These values are similar to the main phase of the ferrihydrite.

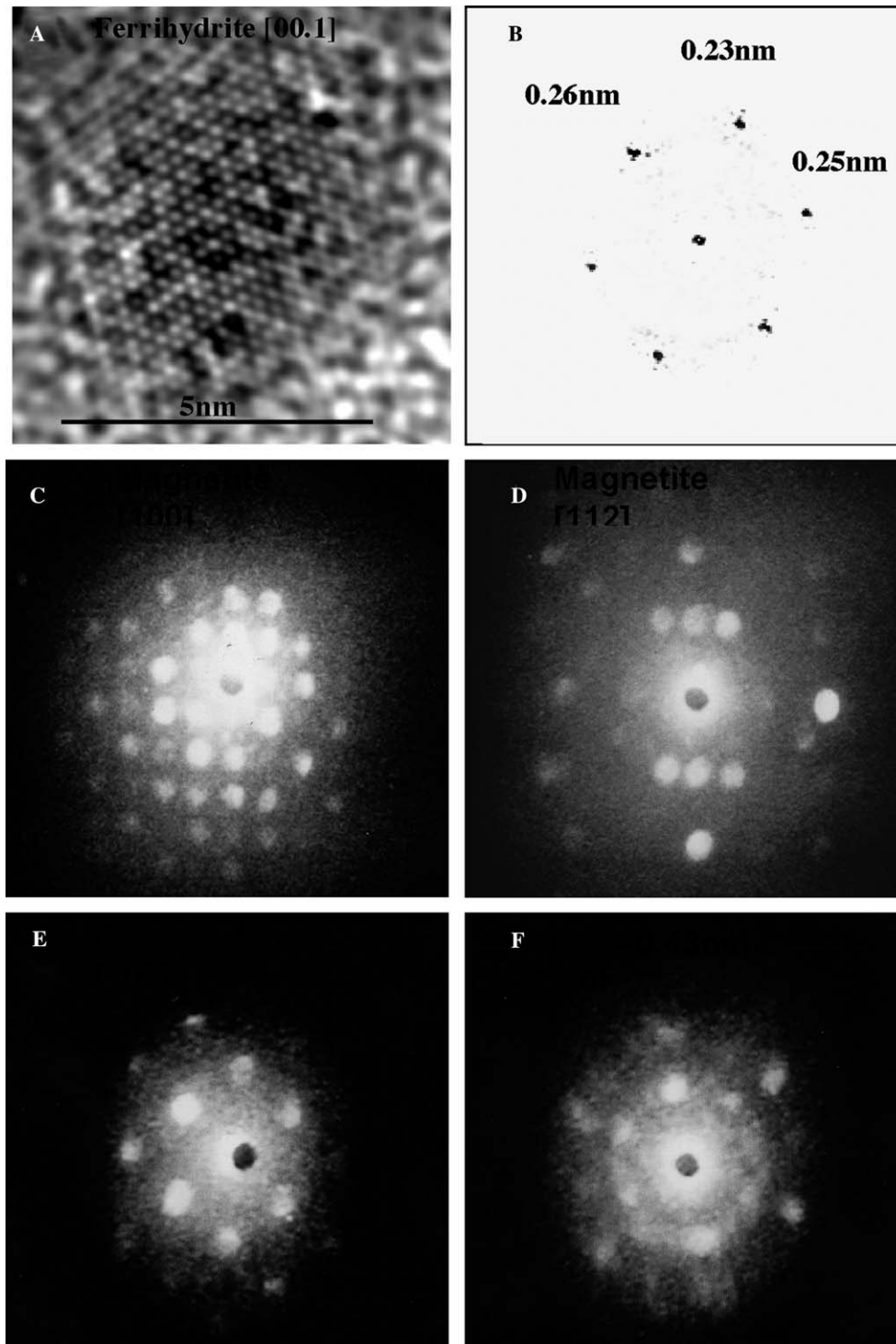


Fig. 5. Human brain ferritin extracted from patients with PSP and AD. (A) HRTEM images of a nanocrystal core. (B) Digital diffractogram of the nanocrystals. (C–F) Electron nanodiffraction patterns from the cubic phases in ferritin from PSP or PHF patients. (C) Magnitite-like phase in [1 0 0] orientation. (D) Magnetite-like phase in [1 1 2] orientation. (E) fcc, $a = 0.43$ nm, phase in [1 0 0] orientation. (F) fcc, $a = 0.43$ nm, phase in [1 1 0] orientation showing continuous lines due to faults on (1 1 1) planes.

Hematite and two cubic phases, one magnetite/maghemite phase and one minor fcc with $a = 0.43$ nm phase, are also present. Ferritin cores normally contain one monocrystal and, consequently, the different structures do not coexist within the same core.

The polyphasic origin of ferritin cores is unknown. It has been suggested, Cowley et al. (2000), that “the mineral phase can be determined by the chemical environment or by the specific form and function of the nucleation sites. The chemical environment seems the

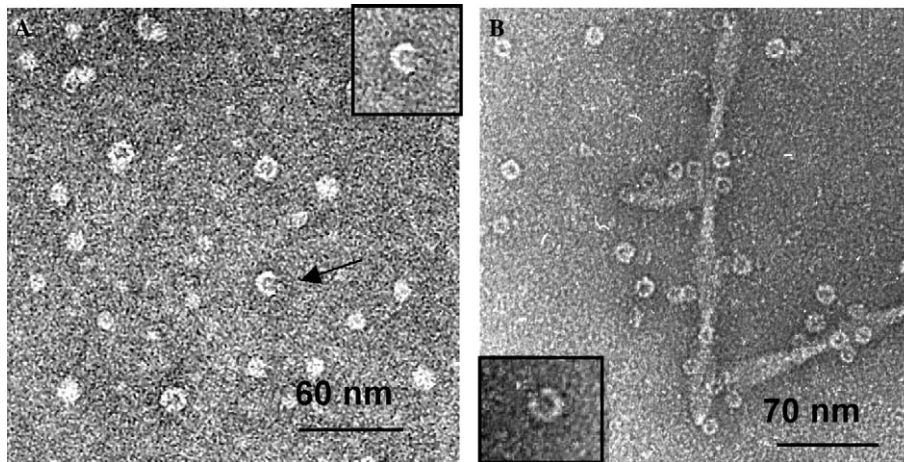


Fig. 6. Human brain ferritin extracted from patients with PSP and AD. (A) PSP ferritin associated to aberrant Tau filaments. Negative stained preparation showing the irregular and incomplete shape of some molecules (hemosiderine). (B) AD ferritin associated to PHF. Negative stained preparation showing the irregular and incomplete shape of some molecules (hemosiderine).

main determinant since it is possible to grow the magnetite phase inside the apoferritin, derived from physiological ferritin molecules, under laboratory controlled conditions (Meldrum et al., 1992).” Under natural conditions ferrihydrite typically forms where oxidation of Fe^{2+} is rapid, in soils containing organic materials that inhibit the formation of more crystalline iron oxides and in soils that are subject to periodic reduction and oxidation (Jambor and Dutrizac, 1998). The mineral is unstable and given time it will convert to more stable iron oxides, namely goethite and hematite (Schwertmann et al., 1999). The transformation can be retarded by adsorption of various species, both inorganic and organic. The existence of several iron oxides in normal ferritin could represent different forms of iron storage: One more labile form, the ferrihydrite, allowing a rapid release of the iron, and an other more stable form represented by the hematite. The cubic forms that are present could be intermediate phases (Campbell et al., 1997).

The ferritin cores from the brain of the aged healthy subject, “in situ” analyzed, differ from the physiological ferritin cores of horse spleen and human liver. Although the ferrihydrite is the major phase, there is a higher proportion of the fcc structure with $a = 0.43$ nm.

The ferritin cores from the brains of patients suffering neurodegenerative diseases differ significantly from the physiological ferritin cores obtained from different sources. The main differences observed are: ferrihydrite is now a minor component and the main component is the fcc structure with $a = 0.43$ nm; the magnetite/maghemite phase is present in similar proportion in all the analyzed ferritin cores.

The fcc phase with $a = 0.43$ nm has a structure which appears to be similar to that of wüstite, Fe_{1-x}O , the mineral in which, as in magnetite, iron is found in two valence states Fe^{3+} and Fe^{2+} . Definite identification

with wüstite is avoided because no clear evidence for the composition, FeO , can be found. It is not possible, with present instrumentation, to obtain both electron nanodiffraction patterns and accurate microanalysis from individual ferritin cores. Many of the cores giving patterns from this structure in the $[110]$ orientation, show strong continuous streaks between the (111) and (200) -type spots, often with diffuse intermediate intensity maxima along the streaks, as seen in Fig. 5F. This is clear evidence for a high density of stacking faults on (111) -type planes. Also, the main spots in the diffraction patterns are often rather diffuse, denoting further disorder in the structure. It is possible that the faults in the structure are associated with chemical inhomogeneities, such as the occurrence of OH ions. The fact that the unit-cell dimension shows wide variation, from about 0.41 nm to 0.45 nm, is also suggestive of compositional variations. The possibility that this phase may actually be cuprous oxide, which is fcc with $a = 0.42$ nm, produced by oxidation of the contaminating copper particles, is discounted because the occurrence of this structure in the various samples shows no correlation with the occurrence of the copper particles, and because the relative intensities of the spots are sufficiently different from those of a FeO -type structure to allow the distinction to be made in most cases.

The magnetite-like phase generally showed clear diffraction patterns with very little evidence of disorder. The electron nanodiffraction studies showed no evidence for differences of structure at the surfaces of the cores. This suggests that any major modifications of the structure at the surfaces must be confined to a layer less than about 1 nm thick or else involve highly disordered or near-amorphous structures.

Furthermore, in addition to the differences found among cores, we have found variations in the protein shell of ferritin of the PSP and AD patients, both at the

level of shape and peptide composition (PSP patients) suggesting that, beside ferritin, a form of hemosiderin can be present in these patients. Additionally, hemosiderin is “in situ” observed in lysosomes of glial cells in caudata nucleus sections in a PSP patient.

Hemosiderin that is considered as a partial proteolytic product of the ferritin (Weir et al., 1984a) is the second iron storage molecule. It is present in pathological iron overload (Hirsh et al., 2002; Selden et al., 1980), mainly in liver primary hemochromatosis (PH) and spleen or liver secondary hemochromatosis (SH) and in the central nervous system (CNS) in superficial siderosis disease (Durieux et al., 1999), in neuroblastoma cells (Iancu, 1989) and in cerebral cavernous angioma (Vymazal et al., 2000). The hemosiderin cores present in human liver of PH patients are formed by a mixture of two phases: a minor ferrihydrite phase (about 20%) and a major, poorly crystallized phase (Dickson et al., 1988; Mann et al., 1988) with reticular distances at 0.249, 0.212, and 0.153 nm *very near* to d_{111} (0.248 nm), d_{200} (0.215 nm), and d_{220} (0.152 nm) of the fcc structure with $a = 0.43$ nm. The hemosiderin shell is thinner than the ferritin shell, irregular and often incomplete (Weir et al., 1984b, 1985). Analysis of peptides present in hemosiderin molecules shows bands between 12.9 and 17.8 kDa significantly smaller than ferritin (20 kDa) (Ward et al., 1994; Weir et al., 1984b).

The structural differences of the pathological ferritin cores suggest that mineralization is altered. Moreover, an important number of crystals present defects. This could mean that the mineralization process can be perturbed not only by modifications in the chemical nature or geometry of the environment, but also *by dysfunction of some steps during the crystal nucleation or growth*. Accordingly, the presence of mineral cubic phases magnetite-like and wüstite in which ferric and ferrous iron ions are both present would indicate that the enzymatic oxidation of iron inside ferritin was faulty (Quintana et al., 2000). The absence of Hm (that is highly stable), its replacement by a magnetite-like and wüstite phases are consistent with an easier mobilization of Fe in these abnormal ferritins. Increase of unbound ferrous ions in cytoplasm may contribute to the production of free hydroxyl radicals and thus to cell neurodegeneration through the damage induced in nucleic acids, lipids and proteins.

Consequently, in spite of the limited number of patients analyzed, our results point to a dysfunction of the ferritin (eventually including degradation to hemosiderin) associated to PSP and AD degenerative diseases.

Ferritin dysfunctions in neurodegenerative diseases has been previously reported. Connor et al. (1995), found that the balance of H/L isoferritins was influenced by age, brain region and disease state in Parkinson and Alzheimer diseases: in frontal cortex in AD the H/L ratio is fivefold increased. Mutations in the gene that encode

L ferritin subunit polypeptide have been found associated to neuroferritinopathy (Curtis, 2001). Patients with this neuronal disorder have abnormal aggregates of iron and ferritin in the brain. It has been suggested that incorporation of mutant L subunit into ferritin heteropolymers could compromise the structure and function of ferritin leading to the spontaneous release of highly toxic iron in the neurones and hence oxidative stress and neuronal cell death (Curtis, 2001; Ke and Qian, 2003). Also, Dobson (2001) suggests that “the magnetite inside the ferritin protein cage may act as a precursor for the formation of biogenic magnetite in humans, perhaps through excess loading of iron in the core and the breakdown of normal protein function.” The biogenic magnetite observed in tissues of brain by Dobson’s group has a wide range of size of particles, between 200 nm and a few tens of nanometers; the larger particles have only been observed in tissues extracts but 5–10 μm cluster of finer opaque particles have been observed by optical microscopy in slices, (Dunn et al., 1995). We have not observed magnetite/maghemite particles of micron dimension in our thin sections. Nevertheless, the clusters of hemosiderin that we have found in lysosomes of glial cells can attain 0.5 μm and it is not excluded that they could be related to the finer particles observed in slices by Dunn et al. (1995), showing magnetic properties. If this were the case and as hemosiderin is a partial proteolytic product of the ferritin, our results would appear as a preliminary confirmation of the hypothesis put forward by Dobson (2001).

The use of new high-sensitivity, analytical methods, such as electron nanodiffraction, HRTEM, and different spectroscopies, including nuclear magnetic resonance, magnetometry, etc., can open new avenues when applied either alone or in combination, to study iron brain metabolism for the early diagnosis of neurodegenerative diseases. Vymazal et al. (2000) indeed, have reported that “it appears that it is possible to separate the ferritin, from hemosiderin, containing tissues using in vivo magnetic resonance images (MRI).” These authors “believe that ferritin form of iron is mainly present under normal conditions and that hemosiderin appears more often in disease.” Our results on PSP and AD patients seem to confirm this finding. Hautot et al. (2003) using highly sensitive superconducting quantum interference device (SQUID) magnetometry, have recently reported that the concentration of magnetite is significantly higher in three samples of AD tissues than in aged tissues brain controls.

In conclusion, we believe that our results provide new arguments to support the hypothesis that the disruption expression of iron metabolism proteins, in particular the main iron storage protein, ferritin, induced by genetic or non-genetic factors in neurodegenerative diseases, can be a cause of the increased concentration of brain ferrous toxic iron.

Acknowledgments

This work has been partly supported by Grants PB96-0818 from the Dirección General de Enseñanza Superior (Spain), 08.5/0018/1997 from the Comunidad de Madrid (Spain) and BMC2002-00996. Authors express gratitude to Drs. J Avila, M. Perez, and J. Martin-Benito for sample supplying and preparation, to Prof. Mendiola for helpful discussions about crystallography and Dr. Gonzalez Carreño for providing the horse spleen ferritin (Sigma). The nanodiffraction and EELS studies with the dedicated STEM instruments were supported by the Center for high-resolution electron microscopy at Arizona State University. We are grateful to Dr. Peter Crozier of the Center for Solid State Science, ASU, for doing the EELS analysis of a number of the ferritin cores. C.Q express sincere gratitude to Dr. JL Carrascosa for his encouragement and support.

References

- Bartzokis, G., Cummings, J., Perlman, S., Hance, D.B., Mintz, J., 1999. Increased basal ganglia iron levels in Huntington disease. *Arch. Neurol.* 56, 569–574.
- Brady, G.W., Kurkjian, C.R., Lyden, E.F., Robin, M.B., Saltman, P., Spiro, T., Terzis, A., 1968. The structure of an iron core analog to ferritin. *Biochemistry* 7, 2185–2192.
- Brooks, R.A., Vymazal, J., Goldfarb, R.B., Bulte, J.W., Aisen, P., 1998. Relaxometry and magnetometry of ferritin. *Magn. Reson. Med.* 40, 227–235.
- Burdo, J.R., Connor, J.R., 2003. Brain iron uptake and homeostatic mechanisms: an overview. *BioMetals* 16, 63–75.
- Campbell, A.S., Schwertmann, U., Campbell, P.A., 1997. Formation of cubic phase on heating ferrihydrite. *Clay Miner.* 32, 615–622.
- Chasteen, N.D., Harrison, P., 1999. Mineralization in ferritin: an efficient means of iron storage. *J. Struct. Biol.* 126, 182–194.
- Connor, J.R., Snyder, B.S., Arosio, P., Loeffler, D.A., LeWitt, P., 1995. A quantitative analysis of isoferritins in select regions of aged Parkinsonian and Alzheimer's disease brains. *J. Neurochem.* 65, 717–724.
- Connor, J.R., Milward, E.A., Moalem, S., Sampietro, M., Boyer, P., Percy, M.E., Vergani, C., Scott, R., Chorney, M., 2001. Is hemochromatosis a risk factor for Alzheimer's disease? *J. Alzheimer's Dis.* 3, 471–477.
- Cowley, J.M., Janney, D., Gerkin, R.C., Buseck, P.R., 2000. The structure of ferritin cores determined by electron nanodiffraction. *J. Struct. Biology.* 131, 210–216.
- Curtis, A.R.J. et al., 2001. Mutation in the gene encoding ferritin light polypeptide causes dominant adult-onset basal ganglia disease. *Nat. Genet.* 28, 350–354.
- Dexter, D.T., Carayon, A., Javoy-Agid, F., Agid, Y., Wells, F.R., Daniel, S.E., Jeess, A.J., Jenner, P., Marsden, C.D., 1991. Alterations in the levels of iron, ferritin and other trace metals in Parkinson's diseases and other neurodegenerative diseases affecting the basal ganglia. *Brain* 114, 1953–1975.
- Dickson, D.P.E., Reid, N.M.K., Mann, S., Wade, V.J., Ward, R.J., Peters, T.J., 1988. Mössbauer spectroscopy, electron microscopy and electron diffraction studies of the iron cores in various human and animal hemosiderins. *Biochem. Biophys. Acta* 957, 81–90.
- Dobson, J., 2001. Nanoscale biogenic iron oxide and neurodegenerative disease. *FEBS Lett.* 496, 1–5.
- Dobson, J., Grassi, P.P., 1996. Magnetic properties of human hippocampus tissue. Evaluation of artefact and contamination sources. *Brain Res. Bull.* 39, 255–259.
- Drits, V.A., Saharov, A.L., Salyn, A.L., Manceau, A., 1993. Structural model for ferrihydrite. *Clay Miner.* 28, 185–207.
- Dunn, J.R., Fuller, M., Zoeger, J., Dobson, J., Heller, F., Hammann, J., Caine, E., Moskowitz, B.M., 1995. Magnetic material in the human hippocampus. *Brain Res. Bull.* 36, 149–153.
- Durieux, A., Flocard, F., Ferreira, A., Azulay, J.P., Felten, O., Navarro, V., Chedru, F., Pouget, J., Bequet, D., Clavelou, P., 1999. Superficial siderosis of the central nervous system. *Rev. Neurol. (Paris)* 155, 201–207.
- Eggleton, R.A., Fitzpatrick, R.W., 1988. New data and a revised structural model for ferrihydrite. *Clays Clay Miner.* 36, 111–124.
- García de Ancos, J., Correas, I., Avila, J., 1993. Differences in microtubule binding and self association abilities of bovine brain tau isoforms. *J. Biol. Chem.* 268, 7976–7982.
- Greenberg, S.C., Davies, P., 1990. A preparation of Alzheimer paired helical filaments that display distinct tau proteins by polyacrylamide gel electrophoresis. *Proc. Natl. Acad. Sci. USA* 87, 5827–5831.
- Harrison, P.M., Fischbach, F.A., Hoy, T.G., Haggis, G.H., 1967. Ferric oxyhydroxide core of ferritin. *Nature* 216, 1188–1190.
- Harrison, P.M., Arosio, P., 1996. Ferritins: molecular properties, iron storage and cellular regulation. *Biochem. Biophys. Acta.* 1275, 161–203.
- Hautot, D., Pankhurst, Q.A., Khan, N., Dobson, J., 2003. Preliminary evaluation of nanoscale biogenic magnetite in Alzheimer's disease brain tissues. *Proc. R. Soc. Lond. B—Biol. Lett.* 270, S62–S64.
- Hirsh, M., Konijn, A.M., Iancu, T.C., 2002. Acquisition, storage and release of iron by cultured human hepatoma cells. *J. Hepatol.* 35, 30–38.
- Iancu, T.C., 1989. Iron and neoplasia: ferritin and hemosiderin in tumor cells. *Ultrastruct. Pathol.* 13, 573–584.
- Isaacson, M.S., Ohtsuki, M., 1980. Scanning transmission electron microscopy of small inhomogeneous particles: application to ferritin. *Scan. Electr. Microsc.* 1, 73–80.
- Jambor, J.L., Dutrizac, J.E., 1998. Occurrence and constitution of natural and synthetic ferrihydrite, a widespread iron oxyhydroxide. *Chem. Rev.* 98, 2549–2585.
- Janney, D.E., Cowley, J.M., Buseck, P.R., 2000a. Structure of synthetic 2-line ferrihydrite by electron nanodiffraction. *Am. Mineral.* 85, 1180–1187.
- Janney, D.E., Cowley, J.M., Buseck, P.R., 2000b. Transmission electron microscopy of synthetic 2 and 6-line ferrihydrite. *Clays Clay Miner.* 48, 111–119.
- Janney, D.E., Cowley, J.M., Buseck, P.R., 2001. Structure of synthetic 6-line ferrihydrite by electron nanodiffraction. *Am. Mineral.* 86, 327–335.
- Ke, Y., Qian, Z.M., 2003. Iron misregulation in the brain: a primary cause of neurodegenerative disorders. *Lancet Neurol.* 2, 246–253.
- Kirschvink, J.L., Kobayashi-Kirschvink, A., Woodford, B.J., 1992. Magnetite biomineralization in the human brain. *Proc. Natl. Acad. Sci. USA* 89, 7683–7687.
- Manceau, A., Drits, V.A., 1993. Local structure of ferrihydrite and ferrihydrite by EXAFS spectroscopy. *Clay Miner.* 28, 165–184.
- Mann, S., Bannister, J.V., Williams, J.P., 1986. Structure and composition of ferritin cores isolated from human spleen, limpet (*Patallavulgata*) hemolymph and bacterial (*Pseudomonas arruginosa*) cells. *J. Mol. Biol.* 188, 225–232.
- Mann, S., Wade, V.J., Dickson, D.P.E., Reid, N.M.K., Ward, R.J., O'Connell, M., Peters, T.J., 1988. Structural specificity of hemosiderin iron cores in iron-overload diseases. *FEBS Lett.* 234, 69–72.
- Massover, W.H., 1993. Ultrastructure of ferritin and apoferritin: a review. *Micron* 24, 389–437.
- Meldrum, F.C., Heywood, B.R., Mann, S., 1992. Magneto-ferritin: in vitro synthesis of a novel magnetic protein. *Science* 257, 522–523.

- Morris et al., 1992. Histochemical distribution of non-heme iron in the human brain. *Acta Anat.* 144, 235–257.
- Perez, M., Valpuesta, J.M., Montejo de Garcini, E., Quintana, C., Arrasate, M., Lopez-Carrascosa, J.L., Rabano, A., Garcia de Yébenes, J., Avila, J., 1998. Ferritin is associated with the aberrant Tau filaments present in progressive supranuclear palsy. *Am. J. Pathol.* 152, 1531–1539.
- Qian, Z.M., Shen, X., 2001. Brain iron transport and neurodegeneration. *Trends Mol. Med.* 28, 299–300.
- Quintana, C., Bonnet, N., Jeantet, A.Y., Chemel, P., 1987. Crystallographic study of the ferritin molecule: new results obtained from natural crystals in situ (mollusc oocyte) and from isolated molecules (horse spleen). *Biol. Cell.* 59, 247–254.
- Quintana, C., Lancin, M., Marhic, C., Pérez, M., Martín-Benito, J., Avila, J., Lopez-Carrascosa, J.L., 2000. Initial studies with high resolution TEM and electron energy loss spectroscopy studies of ferritin cores extracted from brains of patients with progressive supranuclear palsy and Alzheimer disease. *Cell. Mol. Biol.* 46/4, 807–820.
- Sampietro, M., Caputo, L., Casatta, A., Meregalli, M., Pellagatti, A., Tagliabue, J., Annoni, G., Vergani, C., 2001. The hemochromatosis gene affects the age of onset of sporadic Alzheimer's disease. *Neurobiol. Aging* 22, 563–568.
- Sayre, L.M., Perry, G., Atwood, C.S., Smith, M.A., 2000. The role of metals in neurodegenerative diseases. *Cell. Mol. Biol.* 46, 731–741.
- Schultheiss-Grassi, P.P., Dobson, J., 1999. Magnetic analysis of human brain tissue. *BioMetals* 11, 67–72.
- Schwertmann, U., Friedl, J., Stanjek, H., 1999. From Fe(III) ions to ferrihydrite and then to hematite. *J. Colloid Interf. Sci.* 209, 215–223.
- Selden, C., Owen, M., Hopkins, J.M.P., Peters, T.J., 1980. Studies on the concentration and intracellular localization of iron proteins in liver biopsy specimens from patients with iron overload with special reference to their role in lysosome disruption. *Br. J. Haematol.* 44, 593–603.
- Smith, M.A., Harris, P.L.T., Sayre, L.M., Perry, G., 1997. Iron accumulation in Alzheimer disease is a source of redox-generated free radicals. *Proc. Natl. Acad. Sci. USA* 94, 9866–9868.
- St. Pierre, T.G., Webb, J., Mann, S., 1989. Ferritin and hemosiderin: structural and magnetic studies of the iron core. In: Mann, S., Webb, J., Williams, R.J.P. (Eds.), *Biom mineralization: Chemical and Biochemical Perspectives*. Verlagsgesellschaft, Weinheim, pp. 295–344.
- Towe, K.M., Bradley, W.F., 1967. Mineralogical constitution of colloidal “hydrated ferric oxides”. *J. Colloid Interf. Sci.* 24, 384–392.
- Vymazal, J., Urgosik, D., Bulte, J.W.M., 2000. Differentiation between hemosiderin and ferritin bound brain iron using nuclear magnetic resonance and magnetic resonance imaging. *Cell. Mol. Biol.* 46/4, 835–842.
- Ward, R.J., Ramsey, M., Dickson, D.P.E., Hunt, C., Douglas, T., Mann, S., Aouad, F., Peters, T.J., Crichton, R.R., 1994. Further characterisation of forms of hemosiderin in iron-overloaded tissues. *Eur. J. Biochem.* 225, 187–194.
- Weir, M.P., Gibson, J.F., Peters, T.J., 1984a. Biochemical studies on the isolation and characterization of human spleen haemosiderin. *Biochem. J.* 223, 31–38.
- Weir, M.P., Gibson, J.F., Peters, T.J., 1984b. Hemosiderin and tissue damage. *Cell Biochem. Funct.* 2, 186–194.
- Weir, M.P., Sharp, G.A., Peters, T.J., 1985. Electron microscopic studies of human hemosiderin and ferritin. *J. Clin. Pathol.* 38, 915–918.